scientific reports

Check for updates

OPEN

Effect of the dry–wet cycle on the mechanical properties of Ili loess with different mica contents

Ji Ma[1,3], Zizhao Zhang[1,2]✉, Runsen Lai[1], Zekun Guo[1], Guangming Shi[1], Yanyang Zhang[1] & Junpeng Huang[1]

The mechanical properties of the loess in the Ili region of China deteriorate significantly when it is subjected to the dry–wet cycles. Attributed to the critical role played by the mica content for the mechanical deterioration of Ili loess, a series of laboratory tests, including the X-ray diffraction (XRD) tests, the triaxial compression tests, the scanning electron microscopy (SEM), and other methods, were carried out to investigate the macroscopic and microscopic properties of Ili loess under different dry–wet cycles (i.e., 0, 1, 3, 5, 10, 15, 20 cycles) and different mica contents (1.8, 3.8, 5.7, and 7.7%). The main research outcomes are as follows: (1) the cohesion of the loess generally exhibits a fluctuating downward trend under different dry–wet cycles, while the internal friction angle of which shows a slight overall upward trend; (2) the content of small particles for the loess with small mica content (1.8%) gradually increases with the increased number of dry–wet cycles, resulting in a loose structure. It is after 20 dry–wet cycles that the clump-like particles with large size was generated. With the increased content of the mica, a large amount of the mica minerals were embedded and interspersed between skeletal particles of the loess in the flaky form; (3) the pore fractal dimension is highly correlated with the cohesion, while both the equivalent particle diameter and equivalent pore diameter are more closely related to the internal friction angle, for which the pore area ratio shows the least correlation with other parameters; and (4) the mica with small values of content will be embedded and interspersed between skeletal particles of the loess, which restricts the relative slippage of the loess mass. However, the increased mica content leads to the oriented arrangements structures in the loess mass, resulting in the occurrence of sliding surfaces associated with the decreased strength.

Keywords Dry–wet cycle, Ili loess, Mica mineral, Microstructure, Macro–micro correlation

Different from the loess widely distributed in the Asia, Europe, North America, and South America, the loess in China is featured with its significant thickness and integrity[1]. In particular, the extensively deposited loess in the Ili River Valley at the western foot of the Tianshan Mountains in China is generally classified into the late Pleistocene Malan loess[2], characterized by its coarse particles, loose structure, relatively large porosity, as well as its high collapsibility[3]. Different from other region, the average annual precipitation of the Ili River Valley ranges from 200 to 550 mm during the April to October[4], the average annual evaporation of which is about 1467.67 mm. Attributed to the frequent alternation of evaporation and rainfall, a large number of geological disasters such as landslides generally occurred within this region. As one of the 17 key geological disaster prevention and control sites in China, it is thus essential to investigate the influence of dry-wet cycles on the mechanical deterioration of Ili loess.

Considering that the mineral composition is always the primary factor controlling the alteration of loess properties, to analysis the property changes of the loess from the perspective of mineral composition is believed to be an effective method[5]. Zhang et al.[6] pointed out that these hydrophilic and expansive minerals will result in the occurrence of landslides, for which the bonding structure between particles will be disrupted attributed to the water absorption. Liu et al.[7] investigated the variation of shear strength of loess samples subjected to different dry-wet cycles and found that the shear strength of the loess is closely related to mineral components. Xu et al.[8] revealed that the dissolution scale of silicate minerals is essentially consistent with the occurrence conditions of

[1]School of Geology and Mining Engineering, Xinjiang University, Urumqi 830017, China. [2]National Key Laboratory of Intelligent Construction and Healthy Operation and Maintenance of Deep-Earth Engineering, Research Base of Xinjiang University, Xinjiang University, Urumqi 830017, Xinjiang, China. [3]Guangdong Provincial Institute of Mineral Resources Exploration, Guangzhou 510000, China. ✉email: zhangzizhao@xju.edu.cn

landslide disasters. Liang et al.[9] suggested that these hydrophilic minerals would lead to the decreased mechanical strength of the loess. Zhao et al.[10] highlighted that the transformation of clay minerals upon the sliding surface is the main reason for the decreased strength of sliding zone soil. Jian et al.[11] indicated that the expansion of clay minerals is one of the critical factors triggling the landslides. All these aforementioned analyses mainly focused on the expansive and hydrophilic minerals, both the arrangement and combination of minerals will promote the sliding. As suggested by Xie et al.[12], the combination of different clay minerals significantly reduces the frictional strength of the sliding zone, which increases the risk of recurrent landslides in turn.

The shear strength is generated when the loess is subjected to deviator stress, which is generally regarded as the most critical indicator to evaluate the mechanics of the loess[13]. The deterioration of the loess subjected to dry-wet cycles is one of the significant factors resulting in the instability of the slope instability as well as the failure of engineering structure. Aldaood et al.[14] found that the dry-wet cycles can lead to strength attenuation in artificially improved soil. Ma et al.[15] observed that dry-wet cycles can reduce shear strength and the effective cohesion. Xu et al.[16] conducted a series of conventional triaxial tests and found that both the cohesion and internal friction angle decrease with the increased number of dry-wet cycles. Their research also indicated that the reduction gradually diminishes until reaching a stable value with an exponential decay. Moreover, the shear strength does not exhibited a continuously decrease with the number of dry-wet cycles. Wang et al.[17] discovered that the dynamic strength of compacted loess exhibited an initial decreases and then gradually increases with the number of dry-wet cycles. Hao et al.[18] conducted consolidated drained triaxial shear tests on compacted loess samples and found that the shear strength of the loess decreases initially and then increases, reaching a critical number between 3 and 9 cycles. Zhang et al.[19] found that the wetting-drying process can affect the suction friction angle and reduce the effective friction angle of unsaturated soil. As reported, the reduced shear strength mainly occurs in the early stage of the dry-wet cycles, for which the most significant reduction is observed at the first cycle. Generally, the change tends to stabilize after 3-7 cycles, although the scatters betweeen different researchers are still obvious. Through suction-controlled direct shear tests, it is Chen et al.[20] who found that the influence of the first dry-wet cycle is more significant than subsequent cycles. Wang et al.[21] verified that the cohesion decreases rapidly in the first three dry-wet cycles, with a reduced rate of decrease in subsequent cycles. However, minimal variation was observed in terms of the internal friction angle.

The damage of the internal structural is the other key factor for the loess affected by the dry-wet cycles. Various laboratory tests have successfully demonstrated that the feasibility to investigate the macroscopic changes of the loess from the microscopic structural perspective. Currently, lots of testing methods, such as the CT scanning[22–24], nuclear magnetic resonance technology[25], the scanning electron microscopy (SEM) tests[26,27], as well as the mercury intrusion porosimetry[28], are applied in practice. Yuan et al.[29] suggested that dry-wet cycles lead to microstructural damage of the remolded red soil and believed that the development of the microscopic cracks to fine cracks is the main reason for the deterioration of the macroscopic mechanical properties. Wei et al.[30] investigated the red clay via the nuclear magnetic resonance technology and identified the effects of the intergranular pores and crackson the attenuation of the cohesion. Liu et al.[31] found that dry-wet cycles can cause cyclical swelling and shrinkage of hydrophilic clay minerals in the remolded expansive soil samples associated with the decreased mechanical properties. Fan et al.[32,33] investigated the characteristics of changes in microstructural parameters of unsaturated soil of coal seams under different dry-wet cycles. A large amount of research focus on the impact of individual micro variables on the macroscopic properties of the loess, however, there are multiple micro variables should be accounted for in the engineering practices. On the other hand, the influence of mineral contents are generally considered, while limited research was carried out to explore changes of macroscopic mechanical properties from the perspective of structural arrangement of the mica minerals.

Although many scholars have relatively mature experimental methods for studying the macroscopic properties of soil, however, few studies were carried out to evaluate the influence of mineral composition on the mechanical properties of loess in the Ili River Valley of China under the action of dry-wet cycles. Quantitative analysis of soil microstructure characteristics and revealing the deterioration mechanism of loess shear strength at the microstructure scale should be further investigated. When analyzing the macroscopic and microscopic correlation of soil, most studies only consider the influence of a single microscopic variable on the macroscopic properties of soil. However, multiple microscopic variable characteristic parameters often work together to affect the mechanical properties of soil in practice. When analyzing the correlation between the characteristic parameters of multiple microscopic variables and the macroscopic parameters, the influence of different mineral contents on the soil is still not well considered.

To investigate the effect of dry-wet cycles on the deterioration mechanism of the Ili loess with different mica contents, a series of laboratory tests were carried out. According to the given number of dry-wet cycles (0, 1, 3, 5, 10, 15, 20 cycles), the shear strength parameters, cohesion, and internal friction angle were all obtained by the triaxial compression tests. Subsequently, the SEM tests were conducted on selected loess samples and the quantitative analysis on the microstructure of the scanned images was performed in parallel. Grey relational analysis was then employed to investigate the correlation between the microstructure and macroscopic parameters. It is believed that the research outcomes will contribute to the in-depth understanding of the variation in loess strength resulting the geological disasters, which will also provide the reference to the prevention and control of geological disasters in the Ili valley.

Laboratory experiments

Physical properties of loess samples

The loess samples investigated in the present research were taken from the Haindesayi debris flow valley (The three-dimensional model in the figure is obtained by establishing three-dimensional terrain through ArcGIS software.) in Xinyuan County, China (Fig. 1). The Haindesayi debris flow valley experiences perennial water flow and there are two landslide groups along either side of the valley. The frequent alternating pattern of evaporation

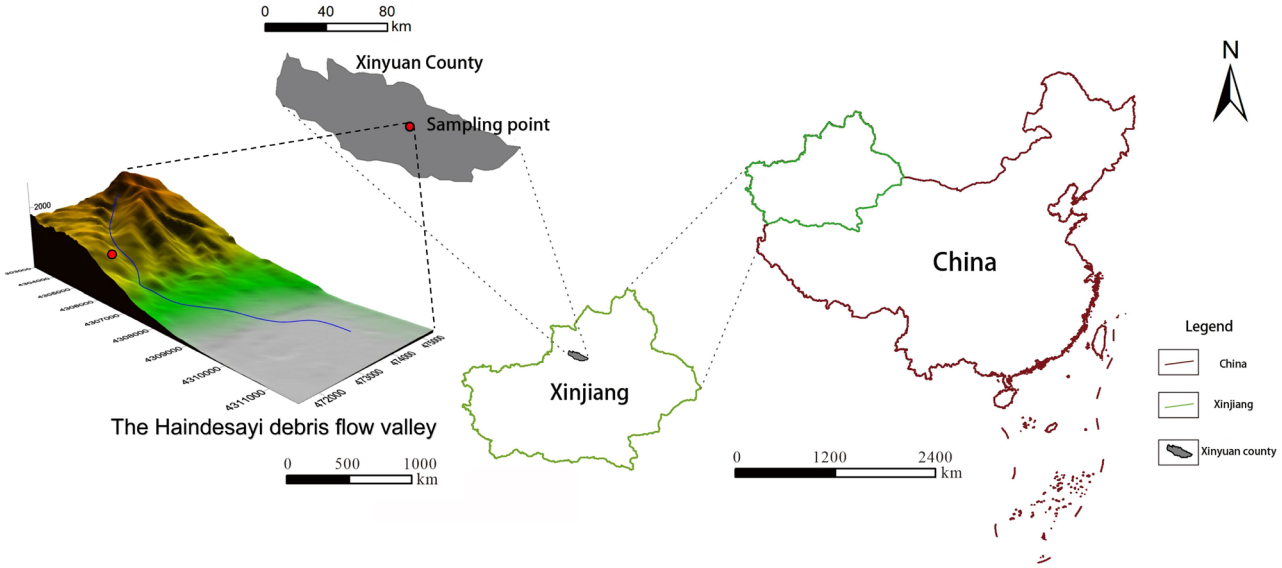

Fig. 1. Sketch of the sampling location.

Natural density (g·cm^{-3})	Natural moisture content (%)	Plastic limit (%)	Liquid limit (%)	Plasticity index	Liquidity index
1.96	18.36	17.53	26.42	8.89	0.09

Table 1. Basic Physical Properties of the loess samples.

and rainfall in this region make it sensitive to dry-wet cycles. Sampling from 2 meters below the surface, these undisturbed loess samples were directly adopted to determine its physcial properties (i.e., density, moisture content, liquid limit, plastic limit, and particle size distribution), the testing results of which are listed in Table 1 for reference. According to the analysis results shown in Table 1, the loess investigated in the present research is a typical cohesive soil.

Experimental design

X-ray diffraction (XRD) test

The loess samples collected from different locations within the debris flow valley (i.e., the foot, the body and the back wall of the landslide) were tested by the X-ray diffraction (XRD) to determine the mineral types and contents. According to the test results, variable mica contents (e.g, 1.8, 3.8, 5.7, and 7.7%) were set up to investigate the influence of mica content on the mechanical behavior of the loess samples subjected to different dry-wet cycles.

Dry-wet cycle tests

To investigate the mechanical behaviour of the loess samples subjected to dry-wet cycles, a total of 28 samples were prepared and divided into 7 groups according to the number of dry-wet cycles (i.e., 0, 1, 3, 5, 10, 15, 20 times). These prepared samples were placed for 24 hours before the conduction of the dry-wet cycle tests. Considering that the moisture content of the loess sampled from the Ili region typically varies between 15 and 20% during the rainy season, the values of moisture content of the loess samples was set at 15–21% as well. The moisture content of the sample was controlled by weighing method, which mainly recorded the mass of 15 and 21 % of the sample. The mass was weighed during the process of humidification and drying to control the moisture content of the sample.

As depicted in Fig. 2, all samples were pre-treated to maintain the constant initial moisture content of 15% and then moistened to the highest moisture content of 21%. The immersion method with an immersion time exceeding 12 hours was adopted herein. Once the target moisture content was reached, the samples will be kept in the laboratory for 10 hours without any additional treatment. Subsequently, a desiccation process was carried out via the simulated lighting system in an oven with a given temperature of 40 °C.to dry the samples to the target moisture content of 15%. After the 10-hour standing period, one dry-wet cycle was completed within 40 hours, for which the moisture content was repeated from 21 to 15%.

Indoor triaxial compression test

The triaxial compression test was conducted with the application of the TFB-1 non-saturated soil stress-strain controlled triaxial apparatus. The samples had a constant diameter of 39.1 mm and a height of 80 mm, respectively. Given the rapid occurrence of geological disasters, the undrained and unconsolidated shear strength test (UU)

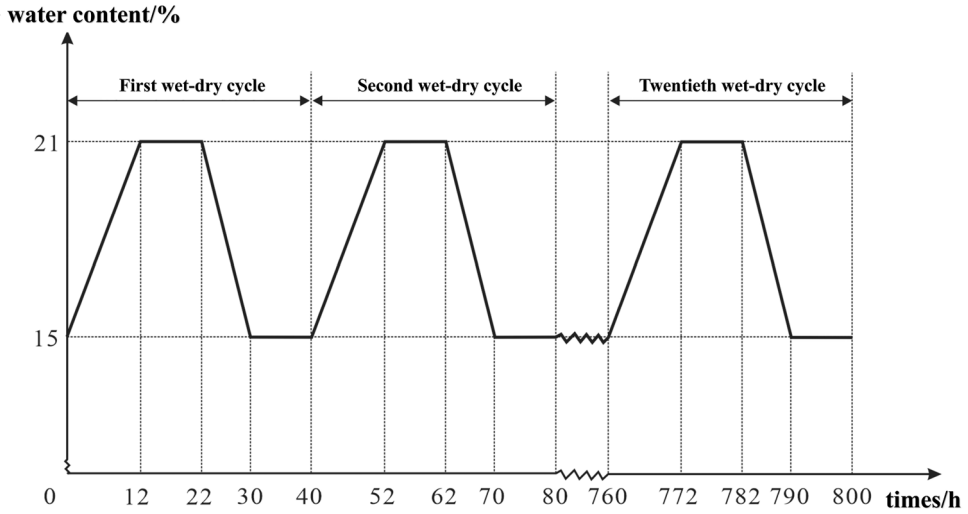

Fig. 2. Process of the dry–wet cycle experiment.

was adopted in the present research, for which variable confining pressures (i.e., 100, 200, and 300 kPa) were applied. Considering that the loess investigated in this study is the cohesive soil, all tests were carried out as per the standard geotechnical testing method and the shear strain rate of which was 0.1% per minute[34].

Scanning electron microscope (SEM) test

The dimensions of samples prepared for SEM tests are 39.1mm x 80mm, which is as same as the samples for triaxial compression test. The cross-shaped layout was chosen to select five points from the representative samples and these points were scanned with different magnifications (i.e., 50x, 200x, 500x, and 800x). It should be noted that a total of 140 points from 28 sets of samples were captured and microscopic qualitative and quantitative analysis will be carried out upon these optimal images.

To better reflect the actual image condition, SEM images at 500x magnification were selected for further processing and quantitatively analysis by the Matlab software and IPP (Image-Pro Plus) image analysis software. As illustrated in Fig. 3, the specific SEM image was read and the label bar of was cropped. Followed by the extraction of the uneven background, the image subtraction and median filtering wew performed. Afterward, the histogram equalization adjustment was applied associated with the threshold adjustment for segmentation. Small noise points were then removed to obtain the binarized image.

Experimental results and analysis

XRD test results

The statistical results of XRD tests are summarized in Fig. 4, which suggests that there are lots of quartz, calcite, feldspar, mica, clay minerals, and dolomite distributed within the loess sample collected for different locations of the landslide. Specifically, the quartz content exhibited a decreasing trend from the foot to the back wall of the landslide. The calcite content in the body and back wall of the landslide was relatively similar, but the values of which are higher than that in the foot samples. The feldspar content experienced an initially increase and then decrease with minor fluctuations in overall. The content of the clay mineral initially decreased and then increased with the elevation. Compared to its counterparts, the dolomite content was relatively low, the values of which ranges from 2 to 5%, with minor overall variations at different locations of the landslide. It can be seen from the results that the mica content increased from 1.8% at the foot to 7.7% in the body and 15.2% in the back wall of the landslide. The possible reason for gradient in mica content is that the downward slide of soil from the top to the foot attributed to the occurrence of the landslide. Meanwhile, the movement of the loess caused by the flowing water should also be accounted for.

It has been found that the mica content will deteriorates the shear strength of the loess[35]. That is, the higher the mica content, the lower the shear strength of the loess, especially within the initial first three dry-wet cycles. To further evaluate the role palyed by the mica, a refined mica gradient approach was adopted in the present research. Considering the mica content of Ili loess typically ranges from 1.03 to 8.6%[36], the mica content at the back wall of the landslide was not considered. Instead, the mica contents at the foot and the middle of the slope were taken as the baseline and the upper limit. Taking the mica gradient to be 2%, the mica contents investigated in this study are 1.8, 3.8, 5.7, and 7.7%, respectively.

Triaxial compression test results

Upon the triaxial compression tests on these samples subjected to the dry-wet cycles, the strength envelopes of the loess samples were established based on the Mohr circles. As depicted in Fig. 5, both the cohesion and internal friction angle of these samples with variable mica contents were calculated. It is apparent in Fig. 5a that the cohesion of the loess samples with different mica contents shows an obvious decrease associated with significant fluctuations, when the number of dry-wet cycles increased. In particular, there is a more pronounced

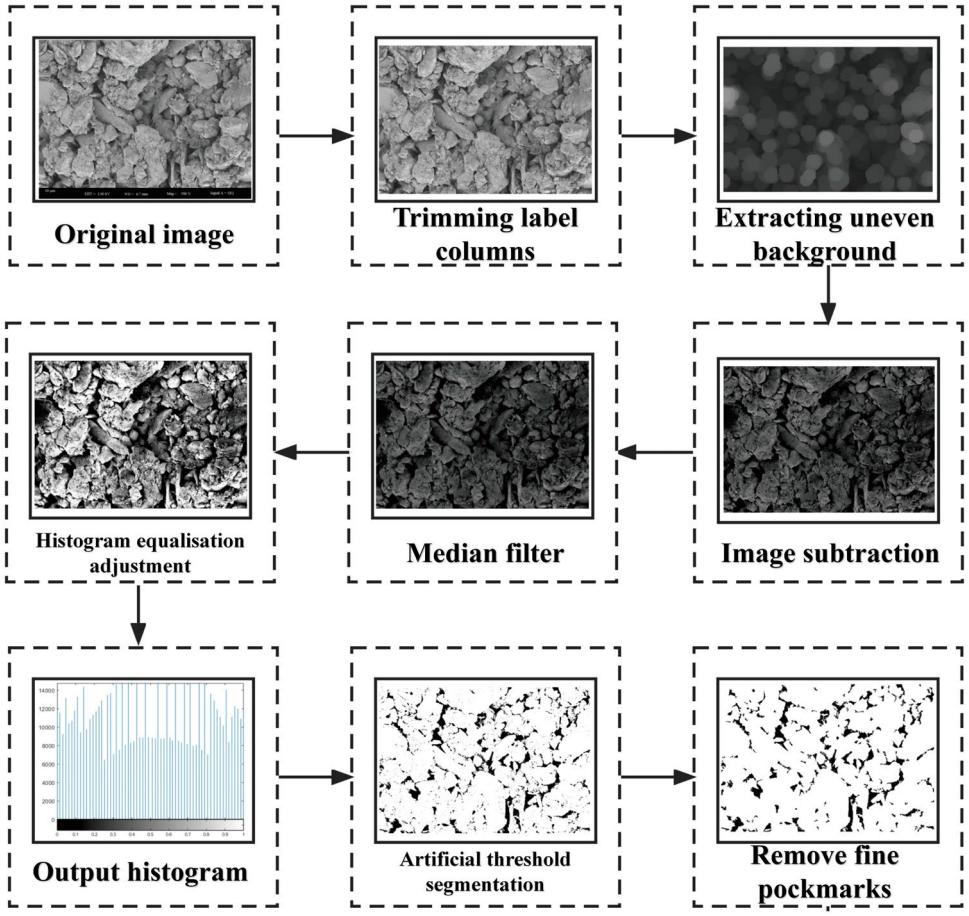

Fig. 3. Process flowchart of microscopic image processing.

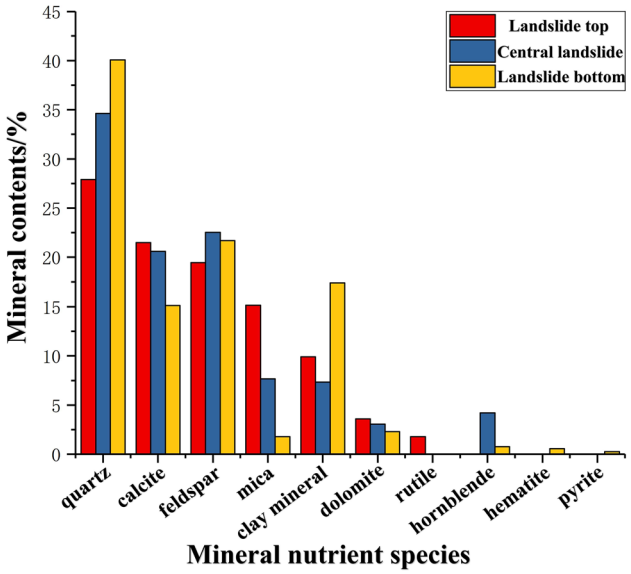

Fig. 4. Mineral types and contents at different locations of the landslide body.

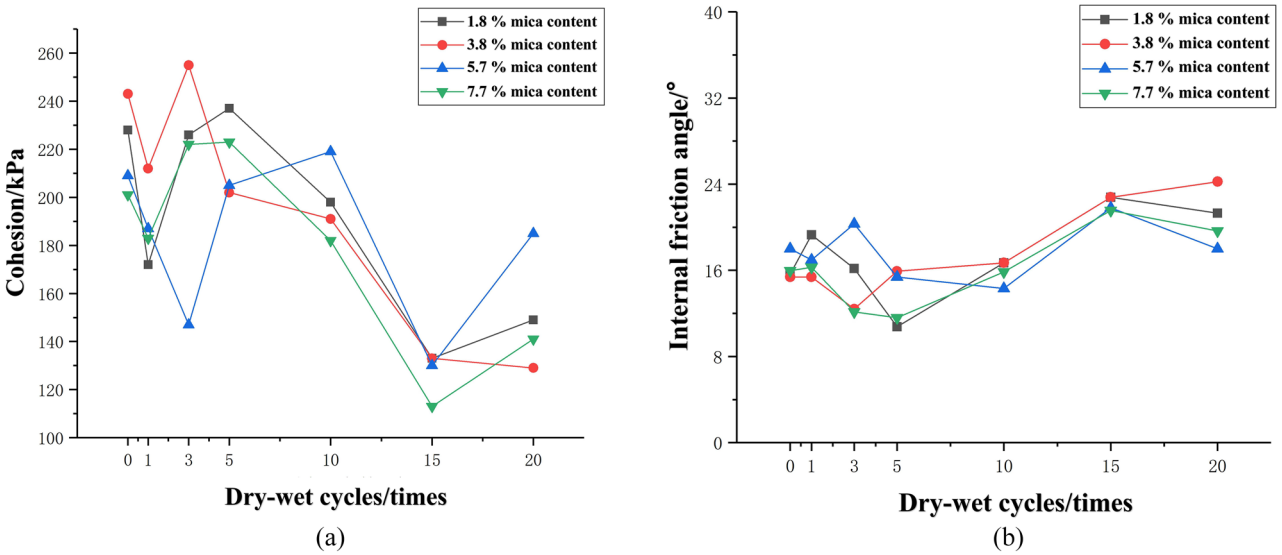

Fig. 5. Variation of shear strength parameters of loess with different mica contents under dry–wet cycles. (**a**) cohesion. (**b**) internal friction angle.

decrease in cohesion for the loess ample with 3.8% mica content. Except for the occasional increases in cohesion during the first three dry-wet cycles, it suffered from the overall decrease with the increased number of dry-wet cycles. It can be seen from Fig. 5a that the cohesion of the soil samples with 1.8, 5.7, and 7.7% mica content shows a "W" shape as the number of dry-wet cycles increase. It is either after the first or the third dry-wet cycles that the first minimum value was achieved, whereas the second minimum value of which was observed after 15th dry-wet cycles. The arrangement of mica minerals will affect the strength of soil structure. The vertical arrangement of mica minerals relative to fissures will strengthen the soil structure, and the same direction with fissures will promote sliding. The curve fluctuation indicates that there is the disturbances occurred within the loess mass and the anisotropy arrangement of mica minerals resulted in an overall decrease in terms of the cohesion.

After the initial dry-wet cycle, the internal space of the soil is disturbed, the spatial structure is destroyed, the soil particles are decomposed into small particles, the pores are enlarged, the mica particles may be arranged in a directional manner, the cementation between the particles is weakened, and the cohesion is significantly reduced. Under the action of subsequent dry and wet cycles, the fine particles decomposed by the particles are filled in the pores, and new cementation is generated between the small particles, and the mica minerals are interspersed and embedded in the pores to form a reinforcement effect, and the cohesion is improved. Overall speaking, the effect of large particles decomposing into small particles is greater than that of small particles cementing each other. As a result, the cohesion shows an overall downward trend.

As depicted in Fig. 5b, the internal friction angle of the loess samples with different mica contents exhibited an increasing trend with increased number of dry-wet cycles, for which the variation is typically between 12° and 24°. Among them, the increased internal friction angle is more pronounced for the loess sample with 3.8% mica content, which is different from the samples with other mica content levels with significant fluctuations. Other loess samples generally exhibited an "M" shape trend characterized by the repeated increase and decrease, suggesting that the dry-wet cycles have a relatively minor impact on the internal friction angle rather than the overall internal friction angle of the loess mass. That is, the cohesion of the loess decrease with an increased number of dry-wet cycles, while the trend in the internal friction angle variation is not as pronounced. This observation indicates that the cohesion is the primary factor resulting in the decreased shear strength of the loess, when it is subjected to the dry-wet cycles.

SEM image analysis

Effect of dry-wet cycles

Herein, the SEM images at 500 times magnification of the loess sample with 1.8% mica content were selected to investigate the microstructure variations of the raw loess sample subjected to different dry-wet cycles. It is obvious in Fig. 6 that the particles of the dense loess sample are mainly aggregated in clusters with large-size cohesive blocks at the initial stage. With the increased number of dry–wet cycles, the number of small particles distributed around pores and particles of the loess mass exhibited an increase. During this period, the particle size of cohesive blocks decreased and the looser soil structure was consequently generated. However, the large cohesive block-like particles were occurred again after 20 dry-wet cycles. These point contacts are mainly the face-to-face contact between particles, which start to transitions to face-to-edge and face-to-point contacts with the increased number of dry–wet cycles. Furthermore, the roundness of soil particles increases with an increase in the number of dry-wet cycles. Moreover, the area of the pores enlarges associated with some cracks with the increase in the number of dry-wet cycles.

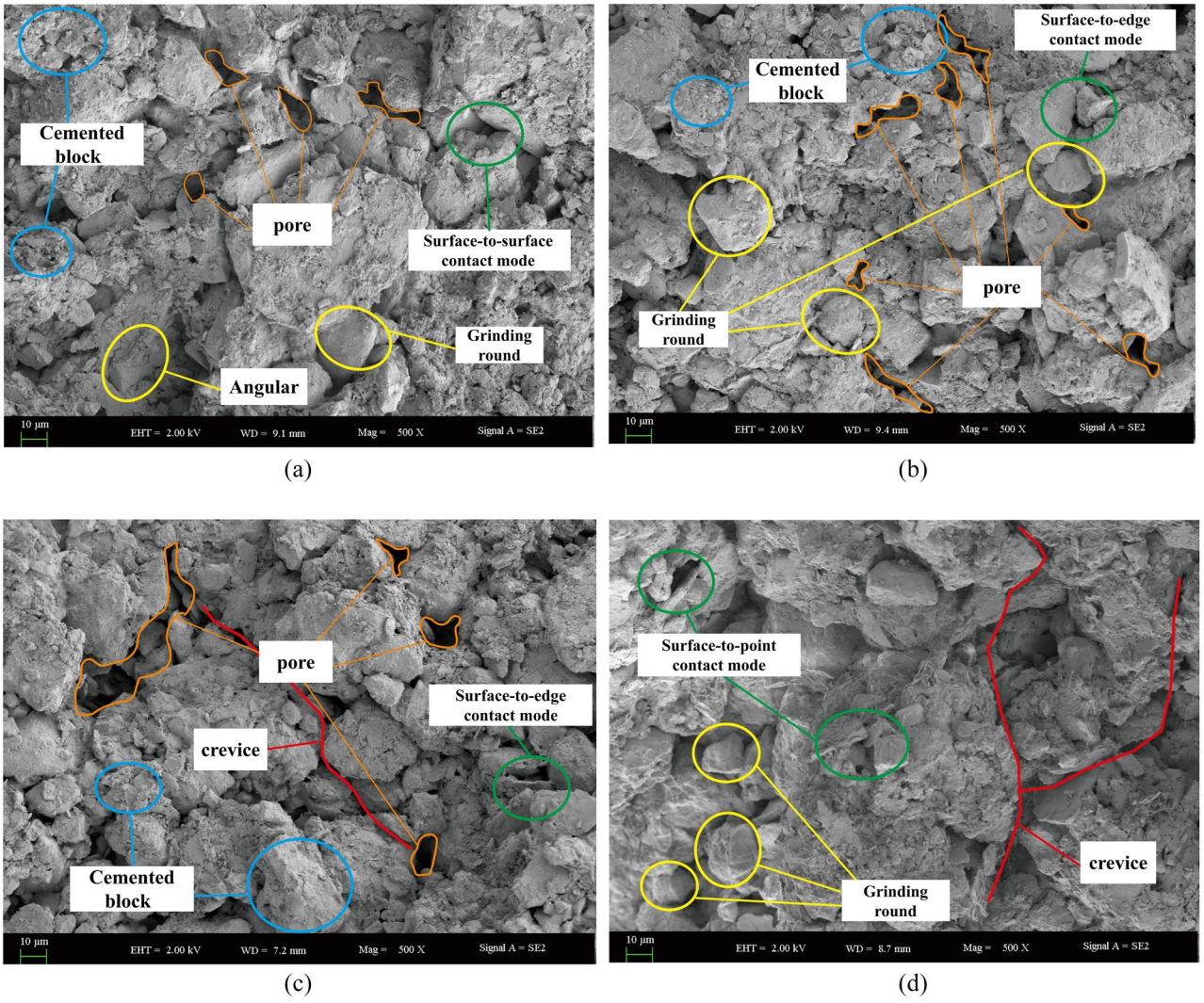

Fig. 6. Microstructure of the Sample with 1.8% Mica in mass. (**a**) 0 dry–wet cycles. (**b**) 3 dry–wet cycles. (**c**) 10 dry–wet cycles. (**d**) 20 dry–wet cycles.

Microstructure variations under different mica contents

Figure 7 compares the loess samples with different mica contents, however, none of which is suffering from the dry-wet cycles. It is apparent that the pores between loess particles are small, and the particles are relatively dense with predominantly face-to-face contacts between them. With an increase in mica content, the loess sample still exhibits a relatively dense structure, although the flake-like mica minerals are embedded and intercalated among the skeletal particles. It can be observed from Fig. 7b that mica minerals are embedded in pores, which reinforces the loess structure and fills the pores in the loess. In addition, mica minerals depicted in Fig. 7c,d are interspersed between soil particles. Because that the mica minerals have a flaky structure and friction between particles, the decreased internal friction angle directly affect the mechanical properties of the loess.

Effect of mica contents

Selection of microscopic characteristic parameters

The information extraction after the image processing is further carried out to obtain the microscopic feature parameters. Herein, the shear strength parameters (e.g, the cohesion and internal friction angle) were selected as the parent sequence. After calculating the average values of the microscopic structural parameters, the pore equivalent diameter, particle equivalent diameter, pore area ratio, particle abundance, pore fractal dimension, as well as the particle fractal dimension were taken as the feature sequence. Followed by the dimensionless of raw data, the grey relational analysis was performed to investigate the macro-microscopic correlation of loess samples with variable mica contents under different dry-wet cycle conditions. Pore equivalent diameter, grain equivalent diameter are used to characterize the size of pores in the soil, while the pore area ratio mainly represents the content of pores in the soil. Note that the grain abundance was adopted to represent the shape of particles, for which the larger abundance generally means that the rounder particles. Herein, the pore fractal dimension and grain fractal dimension were used to represent the roughness of pores and the complexity of the loess

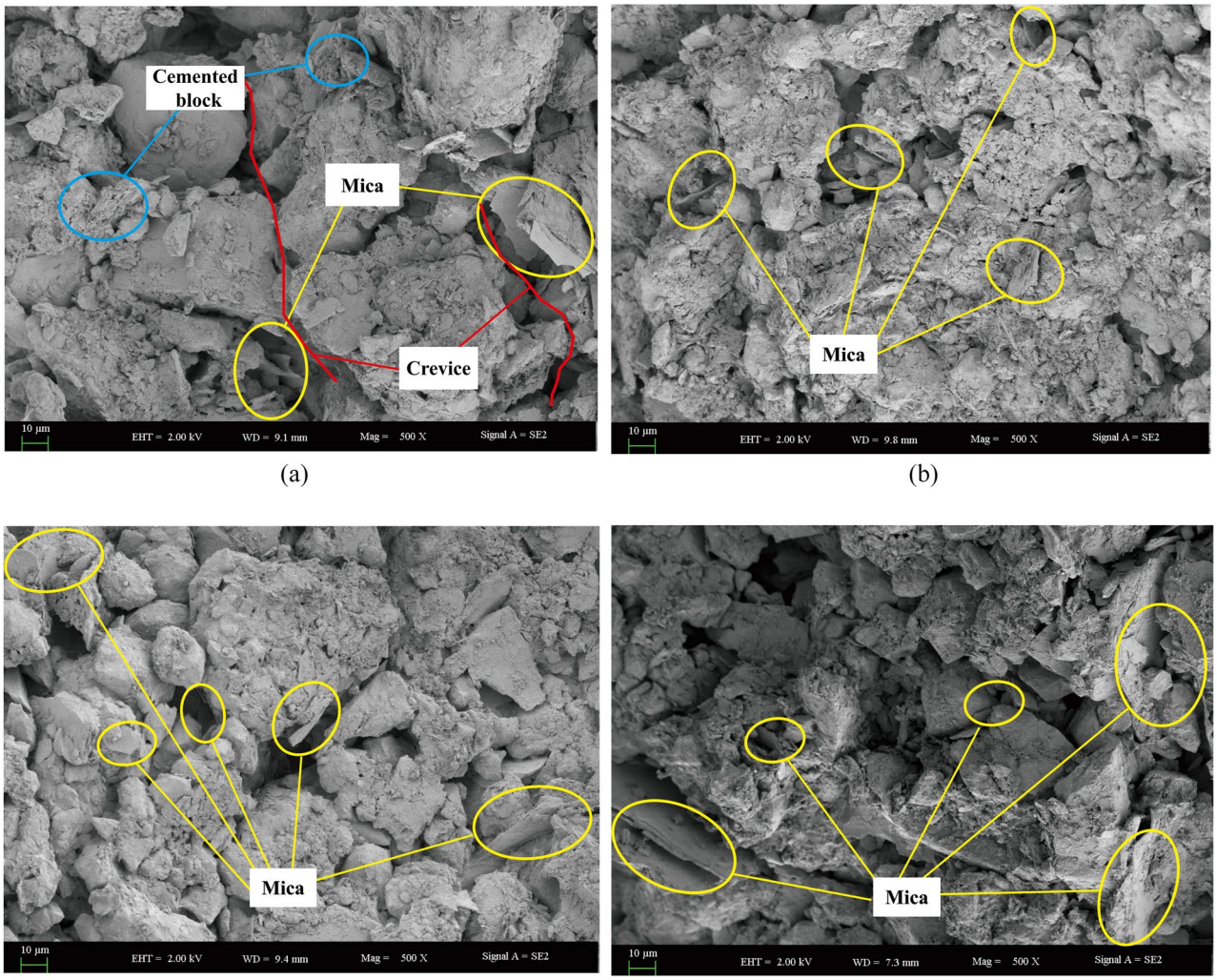

Fig. 7. Microstructure of the natural samples with different mica contents. (**a**) 1.8% mica content. (**b**) 3.8% mica content. (**c**) 5.7% mica content. (**d**) 7.7%mica content.

The change of microscopic characteristic parameters under different mica content

In order to better analyze the influence of different mica content on the microstructure characteristics and mechanical properties of the loess, the microscopic images of different dry-wet cycles were selected for analysis, and the effects of pore equivalent diameter, particle equivalent diameter, pore area ratio, particle abundance, pore fractal dimension as well as the particle fractal dimension on the mechanical properties of loess were analyzed in this section.

Pore equivalent diameter The microscopic pores of the loess are classified into different groups according to the equivalent diameter. The pores in the loess are mostly micro-pores and small pores, for which the micro-pores account for about 20 % and the small pores account for about 70 %. The proportion of macropores is very small, or even does not contain macropores. For loess samples with different mica contents, the number of micropores did not change significantly with the increase of mica content, but the overall increase was observed. The proportion of small pores generally increased first and then decreased, reaching a peak at 3.8 % mica content. The proportion of mesopores and macropores did not change significantly. It shows that the change of mica content on each pore in the soil is uniform. With the increased content of mica, the pore equivalent diameter shows an overall upward trend, and the overall upward trend is obvious. However, the pore equivalent diameter trend of 0.3 and 15 dry-wet cycles is more tortuous (Fig. 8). This phenomenon is mainly attributed to the flaky structure of mica minerals that separates the pores in the loess. As a result, the increased number of micropores and small pores degraded the mechanical properties of the loess.

Equivalent diameter of particles The particles in the loess are also classified into different groups as per the equivalent diameter of the particles. These particles in the soil are mostly fine clay group and colloidal group

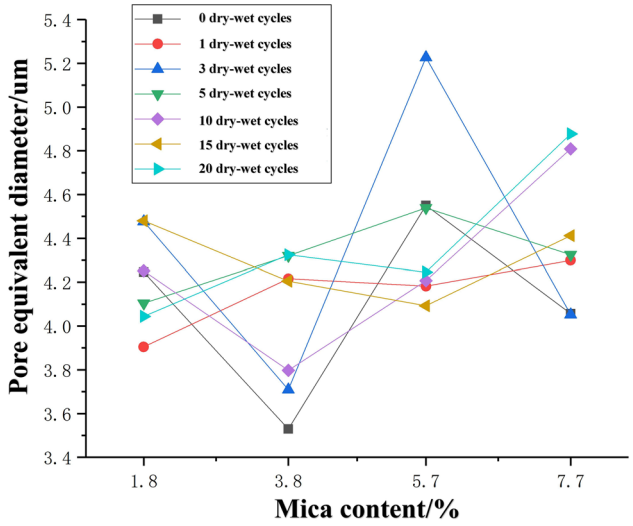

Fig. 8. Relationship between pore equivalent diameter and mica content.

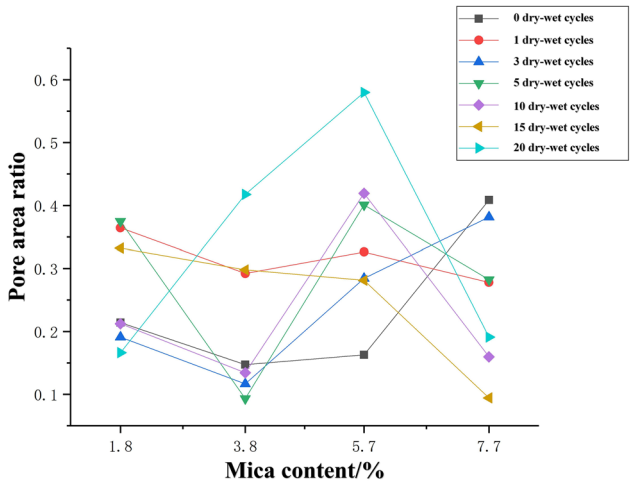

Fig. 9. Relationship between pore area ratio and mica content.

(75-80 %), followed by coarse clay group (>15 %), and other types of particles are less. With the increase of mica content, its change rule is similar to that of pore equivalent diameter.

Pore area ratio With the increased mica content, the pore area ratio of 0 dry-wet cycles decreased initially and then increased, the pore area ratio of 20 dry-wet cycles showed the opposite trend, while the pore area ratio of 15 dry-wet cycles showed a significant downward trend. Under other intermediate dry–wet cycles, the pore area ratio shows a more consistent rule with the increase of mica content, which is first decreased, then increased and then decreased, showing an inverted 'N' type (Fig. 9). It can be seen that the change of pore area ratio is more tortuous, indicating that with the increase of mica content, pore water continuously scours particles under dry-wet alternation, and flaky mica minerals may be washed into pores or blocked pores, so that the change of pore area ratio is fluctuating.

Particle abundance It is apparent that the particle abundance in the loess generally concentrated between 0.3 and 0.7, accounting for more than 15 %. Under different mica content, the overall change of particle abundance is not large. The proportion of 0.4–0.5 interval is the highest under 1.8 % mica content, and the proportion of 0.5–0.6 interval is the highest under other mica content. After adding mica, the proportion of near-circular particles increases, resulting in a decrease in cohesion.

Pore fractal dimension With the increased content of mica, the pore fractal dimension changes more twists and turns, and more shows a downward trend. As can be seen from Fig. 10, water has an effect on soil particles without any mica. With the increase of the number of dry-wet cycles, the distribution of loess particles tends

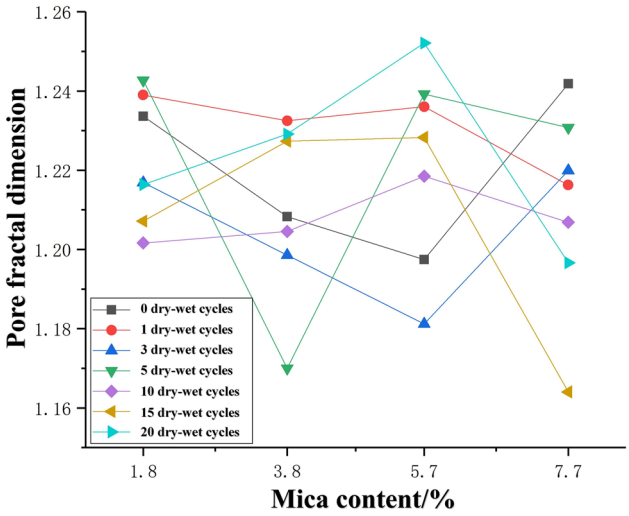

Fig. 10. Relationship between pore fractal dimension and mica.

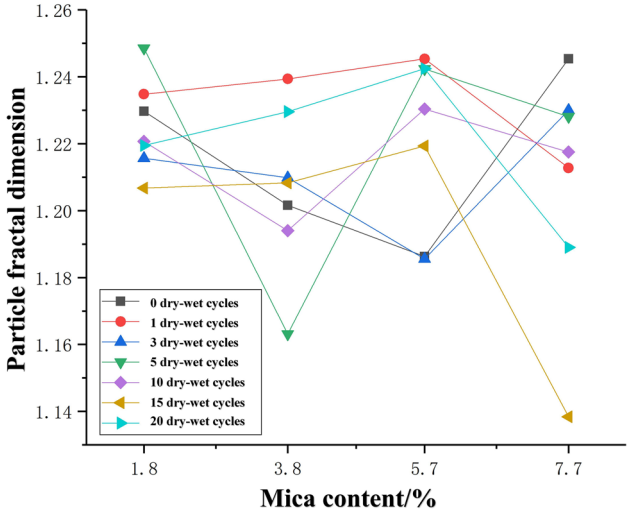

Fig. 11. Relationship between pore fractal dimension and mica.

to be simple, and the pores tend to be simple. When the content of mica is less, the arrangement of mica is disordered and the direction is different under the condition of 0 dry-wet cycle. With the increased number of dry-wet cycles, water has a further effect on the spatial distribution of mica, and the distribution of mica is more complex and disordered. Interspersed and inlaid in the pore space, resulting in a decrease in the fractal dimension of the pore space, making the pore space more orderly. It can be seen from the microscopic images with large block of agglomerated particles and the decrease of cohesion cause the mechanics of loess to deteriorate.

Particle fractal dimension As shown in Fig. 11, with the increase of the number of dry-wet cycles, the fractal dimension of particles changes more twists and turns. Under the conditions of 1 dry-wet cycle, 15 dry-wet cycles and 20 dry-wet cycles, the fractal dimension of particles experienced a downward trend, and the complexity of particles exhibited an initial increase, followed by the decrease until the peak value of 5.7 % mica content was reached. The change rule of the particle fractal dimension discussed herein is similar to the change rule of the pore fractal dimension.

Macro-microscopic correlation analysis

Loess sample with 1.8% mica content Figure 12 depicts the correlation coefficient plots between the parent series cohesion, internal friction angle, and the feature sequence pore equivalent diameter, particle equivalent diameter, pore area ratio, particle abundance, pore fractal dimension for the loess sample with 1.8% mica content. More detailed information are listed in Tables 2, 3 for reference. The calculated results indicated that the correlation coefficients of various parameters with the cohesion for the loess samples are all greater than 0.59, suggesting a close correlation between the pore equivalent diameter, particle equivalent diameter, pore area ratio,

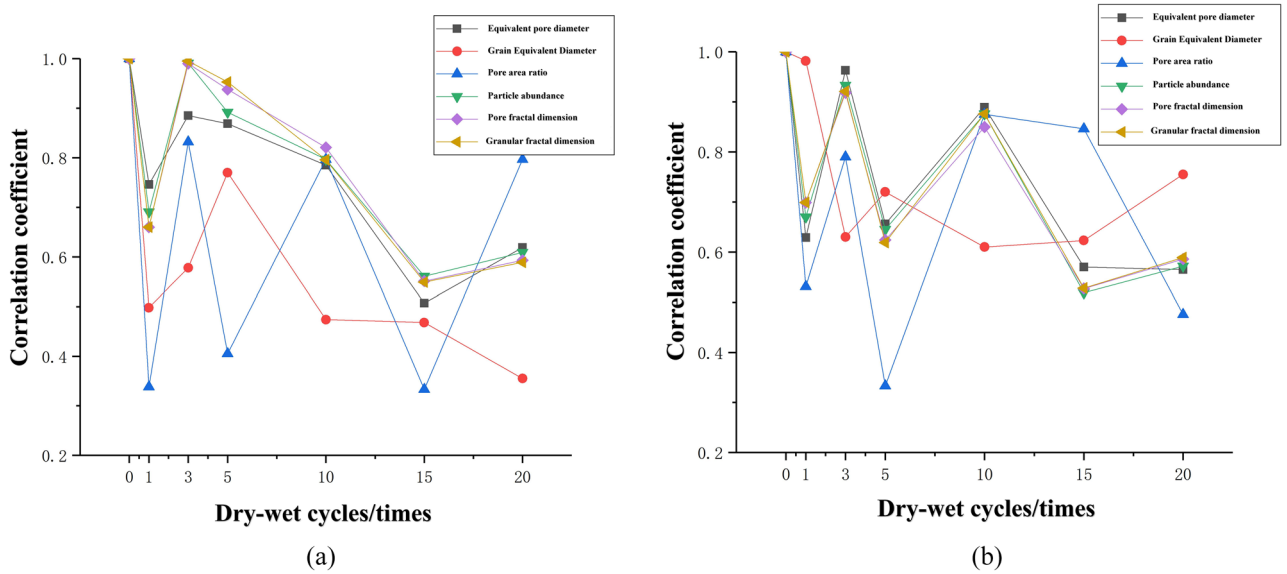

Fig. 12. Correlation Coefficient Plots of Microscopic Characteristic Parameters of Loess with 1.8% Mica. (**a**) cohesion. (**b**) internal friction angle.

Evaluation item	Relatedness	Rankings
Pore fractal dimension	0.793	1
Granular fractal dimension	0.792	2
Particle abundance	0.791	3
Pore equivalent diameter	0.773	4
Pore area ratio	0.643	5
Particle equivalent diameter	0.592	6

Table 2. Correlation results of cohesion of loess with 1.8% mica and microscopic characteristic parameters.

Evaluation item	Relatedness	Rankings
Particle equivalent diameter	0.76	1
Pore equivalent diameter	0.753	2
Granular fractal dimension	0.748	3
particle abundance	0.745	4
pore fractal dimension	0.743	5
Pore area ratio	0.693	6

Table 3. Correlation results of internal friction angle of loess with 1.8% mica and microscopic characteristic parameters.

particle abundance, pore fractal dimension, particle fractal dimension, and the cohesion and internal friction angle of the loess. Among these parameters, the pore fractal dimension shows the highest correlation with the cohesion, while the particle equivalent diameter exhibits the lowest correlation. Regarding the internal friction angle, the particle equivalent diameter has the highest correlation, whereas the pore area ratio has the lowest correlation. It can be seen from Fig. 6a,b that some parameters (i.e., the particle equivalent diameter and pore area ratio) with lower correlation coefficients generally exhibit larger fluctuations.

Loess sample with 3.8% mica content As per the same calculation process presented earlier, the results of loess sample with 3.8% mica content is illustrated in Fig. 13. It is obvious that the correlation coefficients of various parameters with the cohesion and internal friction angle of loess samples are all greater than 0.6. Among them, the particle equivalent diameter shows the highest correlation with the cohesion, while the pore area ratio exhibits the lowest correlation. Corresponding to the internal friction angle, the particle equivalent diameter has the highest correlation, while the pore area ratio has the lowest correlation.

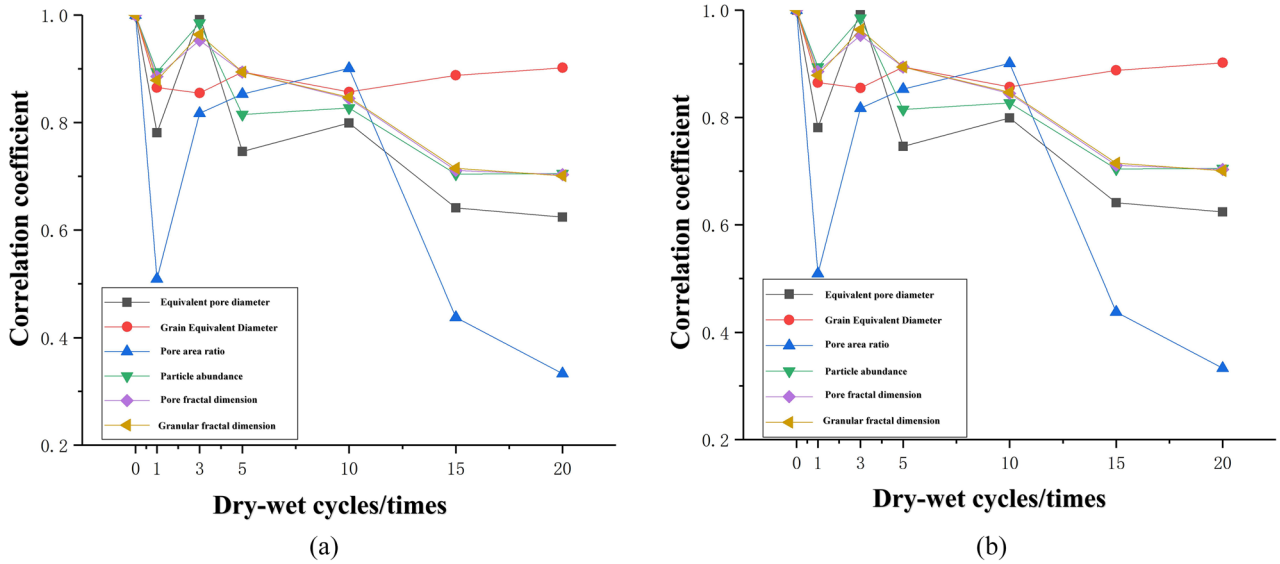

Fig. 13. Correlation Coefficient Plots of Microscopic Characteristic Parameters of Loess with 3.8% Mica Content. (**a**) cohesion. (**b**) internal friction angle.

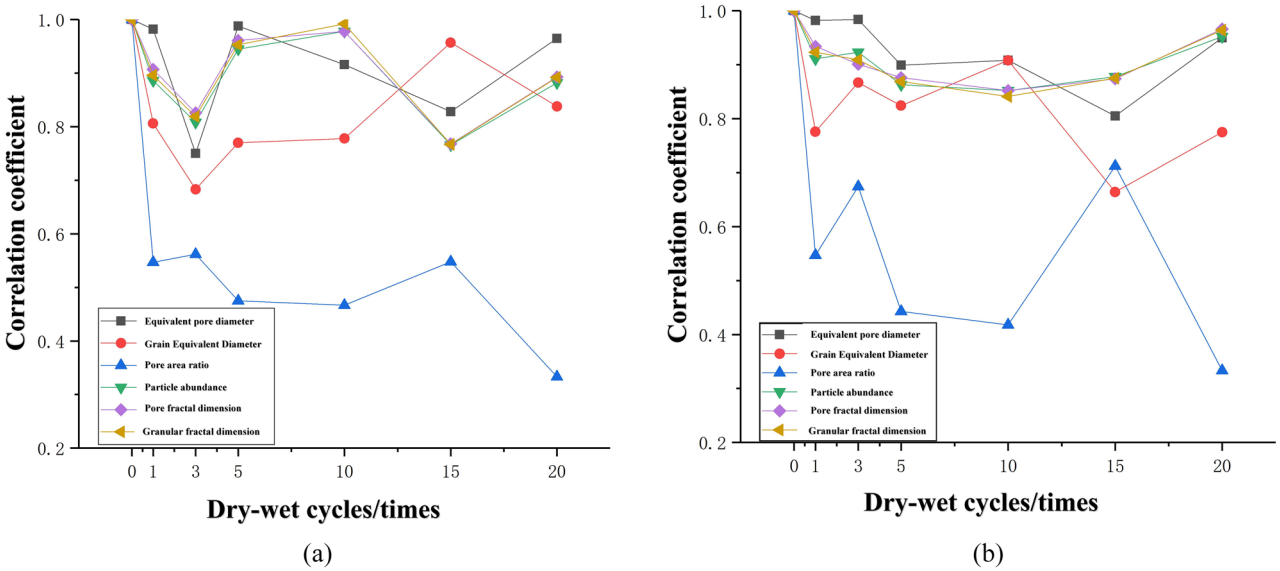

Fig. 14. Correlation coefficient plots of microscopic characteristic parameters of loess with 5.7% mica. (**a**) cohesion. (**b**) internal friction angle.

Loess sample with 5.7% mica content Figure 14 presents the results of the loess sample with 5.7% mica content, suggesting that the pore equivalent diameter shows the highest correlation with cohesion and internal friction angle. Whereas, the pore area ratio demonstrates the lowest correlation with both cohesion and internal friction angle. Except for the pore area ratio, the correlation coefficients of other parameters with the cohesion of loess samples are all greater than 0.6. This observation indicated that there is a close correlation between these parameters and the cohesion and internal friction angle of the loess, while the pore area ratio shows relatively poor correlation with both cohesion and internal friction angle.

Loess sample with 7.7% mica content Figure 15 shows the calculation results of the loess sample with 7.7% mica, which indicates that the particle abundance exhibits the highest correlation with cohesion, while the pore area ratio shows the lowest correlation. Regarding the internal friction angle, the pore equivalent diameter has the highest correlation, and the pore area ratio has the lowest correlation. The correlation coefficients of all parameters with the cohesion of loess samples are greater than 0.6, indicating a close association between these parameters and the cohesion of the loess.

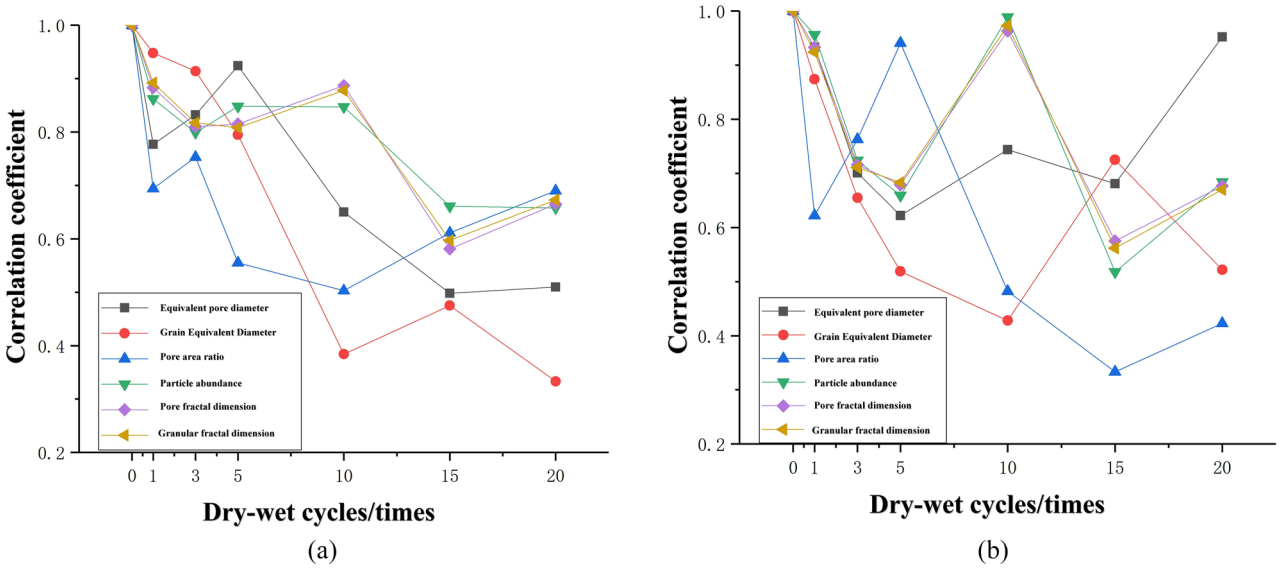

Fig. 15. Correlation coefficient plots of microscopic characteristic parameters of loess with 7.7% mica. (**a**) cohesion. (**b**) internal friction angle.

As discussed above, these parameters highest related with the cohesion generally exhibited the significant variations. It should be noted that the pore fractal dimension shows a significant correlation with the cohesion (>0.8) under different dry–wet cycles. On the other hand, the particle equivalent diameter and the pore equivalent diameter exhibited the highest correlation with the internal friction angle. It is noteworthy that the pore area ratio consistently shows the lowest correlation with the cohesion and internal friction angle, regardless of the mica content.

Discussion

With an increased number of dry-wet cycles, the disrupted structure between particles resulted in the damage of the microscopic structure. As the number of dry-wet cycles increases, the increased content of small particles distributed within the pores or around the particles led to smaller aggregates and a tendency towards a looser soil structure. The predominant face-to-face contact between particles transitions to an increase in face-to-edge and face-to-point contacts, with an increase in point contact forms and roundness of soil particles. Moreover, damage occurs in the microscopic structure of the loess as the number of dry-wet cycles increases. Associated with the enlargement of the pore area, some unexpected cracks may be appeared with the dry-wet cycles.

It is believed that the action of dry-wet cycles damaged the microscopic structure of loess, although there is somewhat fluctuation. Overall speaking, the dry-wet cycles led to a decreased cohesion as well as the shear strength. Because that the loess with maximum dry density generally has a denser microscopic particle structure and lower porosity, the fluctuating changes of various parameters may be attributed to the adoption of the loess samples with the maximum dry density. Additionally, the small magnitude of dry-wet cycle amplitudes in this research did limit the extent of the impact of the dry-wet cycles. Moreover, the evolution process of the loess is inherently complex and the fluctuating changes is normal to some extent. Nonetheless, the overall trend of the changes in the parameters is noticeable in the present research.

As can be seen from Fig. 16a that the Mica, as a layered silicate mineral, typically presents a flaky morphology. When the content of the mica is small enough, the mica particles are thoroughly mixed into the loess and the mica will be embedded and interlaced between the skeletal particles shown in Fig. 16b. This arrangement acts as a reinforcement structure, which exhibits the interlocking interface forces and restricts the relative slippage of the loess mass. In this case, both the strength and overall stability of the loess samples are enhanced. However, for the loess with a large mica contents, the mica particles may align in a directional manner under the vertical pressure. As depicted in Fig. 16c, the distinct slip planeswill result in the decreased strength of the loess mass.

Conclusions

In the present research, the effect of the dry-wet cycle on the mechanical properties of the Ili loess with different mica contents were investigated. With the combination of the tri-axial compression tests and the scanning electron microscopy (SEM) analysis, the relationship between the macroscopic and microscopic properties of the loess samples collected from the typical landslide in the Ili River Valley were set-up. The main research conclusions are as follows:

(1) The cohesion of the Ili loess generally shows a fluctuating decreasing trend under different dry–wet cycles, while the internal friction angle shows little variation associated with an overall increasing trend.

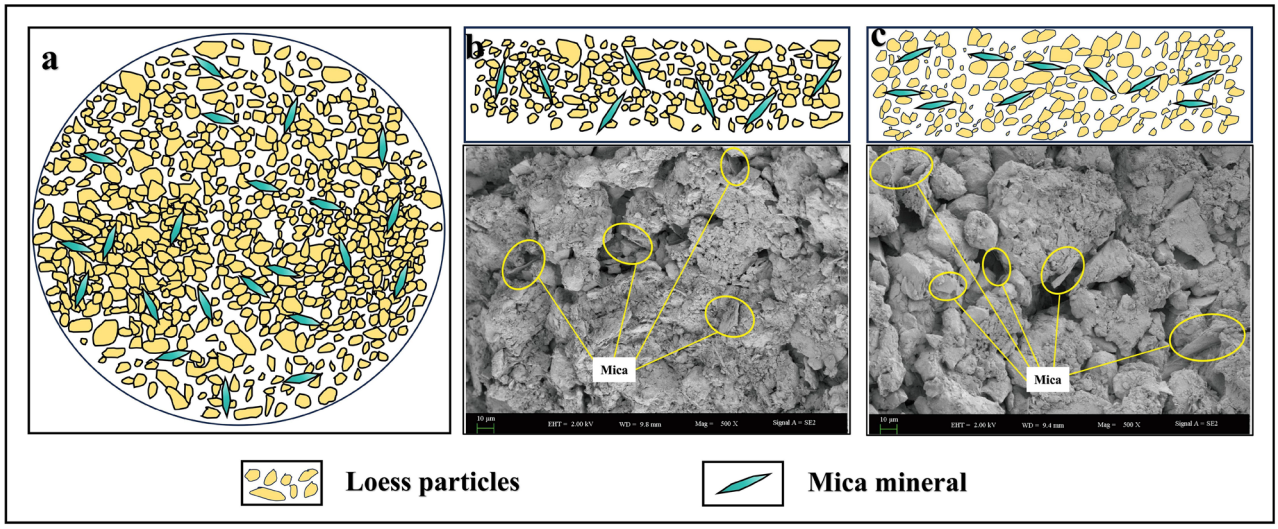

Fig. 16. Role of mica mineral in loess particles.

(2) These small particle distributed within the pores of the loess with low mica content (1.8%) resulted in the looser structure and the occurrence of large size blocks led to an increased roundness of the loess mass after the 20th dry–wet cycle.
(3) With the increased content of the mica, the particle contact of the denser loess is generally in the form of the face-to-face mode and these flaky mica minerals are embedded and interlaced between the skeletal particles.
(4) With the increased dry–wet cycles, the points contact transitions from face-to-face contact to face-to-edge and face-to-point contact.
(5) Compared to other parameters, the pore area is not sensitive to the cohesion and the internal friction angle.
(6) Mica minerals embedded and interlaced between skeletal particles can restrict the relative slippage of the soil mass to some extent.

Data availability

Data availability statement: The datasets used and/or analysed during the current study available from the corresponding author on reasonable request.

Received: 7 September 2024; Accepted: 24 June 2025
Published online: 15 July 2025

References

1. Peng, J. B. et al. The critical issues and creative concepts in mitigation research of loess geological hazards. *Eng. Geol.* **22**(4), 684–691. https://doi.org/10.13544/j.cnki.jeg.2014.04.014 (2014).
2. Song, Y. et al. Distribution and composition of loess sediments in the Ili basin, central Asia. *Quatern. Int.* **334–335**, 61–73 (2014).
3. Guang, Y. I. N. et al. Physical index, dynamic property and landslide of Ili loess. *Arid Land Geogr.* **32**(06), 899–905 (2009).
4. Yi, Liu. *Analysis of Geological Features, Cause and Stability of the Loess Landslide in Ili* (Shihezi University, 2015).
5. Jiang, Yu. & Zhao, Yu. Analysis on formation mechanism of red - stratum landslide based on characteristic mineral. *Yangtze River* **52**(06), 82–87. https://doi.org/10.16232/j.cnki.1001-4179.2021.06.014 (2021).
6. Zhang, S. & Xu, G. Effects of rainwater softening on red mudstone of deep-seated landslide, Southwest China. *Eng. Geol.* **2016**(204), 1–13 (2016).
7. Yuyang, Liu et al. Experimental research on strength and microstructure evolution of Q2 undisturbed loess under different wetting-drying cycle paths. *China J. Highw. Transp.* **35**(12), 168–180 (2022).
8. Zemin, Xu., Runqiu, Huang & Zhengguang, Tang. Kinetics of silicate mineral dissolution and its implications for landslide studies. *Chin. J. Rock Mech. Eng.* **2005**(9), 1479–1491 (2005).
9. Xuezhan, Liang, Hongkai, Chen & Bin, Liu. Analysis of sensitive factors of shear strength parameters of typical soil landslides in three gorges reservoir: A Case study of Qingshi landslide near the Shennv stream. *Inst. Disaster Prev.* **25**(03), 10–17 (2023).
10. Zhao, Yu. & Cui Peng, Hu. Relation between evolution of clay shear strength and landslide induced by acid rain-taking landslides in three gorges reservoir area for example. *Chin. J. Rock Mech. Eng.* **28**(3), 576–582 (2009).
11. Wenxing, Jian et al. Characteristies of incompetent beds in Jurassie red clastie rocks in Wanzhou. *Rock Soil Mech.* **2005**(6), 901–905+914 (2005).
12. Chao, Xie et al. Spectroscopic characteristics of minerals in sliding zone soil in motuo landslides and their engineering significance. *Spectrosc. Spec. Anal.* **36**(7), 2266–2270 (2016).
13. Duncan, J. M., Wong, K. S. & Marby, P. *Stress-Strain and Bulk Modulus Parameters for Finite Element Analysis of Stresses and Movement in Soil Mass* (University of Califomia, 1978).
14. Aldaood, A., Bouasker, M. & Al-Mukhtar, M. Impact of wetting-drying cycles on the microstructure and mechanical properties of lime-stabilized gypseous soils. *Eng. Geol.* **174**, 11–21 (2014).
15. Xuening, Ma. et al. Experimental research on the effect of repeated drying - wetting cycles on the mechanical properties of remolded unsaturated loess. *J. Rail. Eng. Soc.* **39**(01), 1–6+12 (2022).

16. Xu, J. et al. Shear strength and mesoscopic character of undisturbed loess with sodium sulfate after dry-wet cycling. *Bull. Eng. Geol. Environ.* **79**, 1523–1541 (2020).
17. Tiehang, W. et al. Experimental study on dynamic strength properties of compacted loess under wetting-drying cycles. *Chin. J. Rock Mech. Eng.* **39**(6), 1242–1251 (2020).
18. Yanzhou, Hao et al. Structural constitutive relation of compacted loess considering the effect of drying and wetting cycles. *Rock Soil Mech.* **42**(11), 2977–2986 (2021).
19. Fangzhi, Z. & Xiaoping, C. Influence of repeated drying and wetting cycles on mechanical behaviors of unsaturated soil. *Chin. J. Geotech. Eng.* **32**(1), 41–46 (2010).
20. Chen, R. et al. Impact of multiple drying–wetting cycles on shear behaviour of an unsaturated compacted clay. *Environ. Earth Sci.* **77**, 683 (2018).
21. Huan, Wang et al. Analysis of strength characteristics of expansive soil modified with silty sand under dry-wet cycle. *Sci. Technol. Eng.* **21**(26), 11336–11342 (2021).
22. Huang, Zhen et al. Using CT to test the damage characteristics of the internal structure of expansive soil induced by dry–wet cycles. *AIP Adv.* **11**, 075305 (2021).
23. Timing, Wang et al. Evolution of fissures and bivariate - bimodal soil - water characteristic curves of expansive soil under drying-wetting cycles. *Chin. J. Geotech. Eng.* **43**(S1), 58–63 (2021).
24. Shiji, W. et al. Experimental study on crack evolution and strength attenuation of expansive soil under wetting-drying cycles. *Trans. Chin. Soc. Agric. Eng. (Trans. CSAE)* **37**(5), 113–122 (2021).
25. Dong, J. et al. NMR-based study on soil pore structures affected by drying-wetting cycles. *Arab. J. Sci. Eng.* **45**, 4161–4169 (2020).
26. Yongpeng, Nie et al. the influence of drying-wetting cycles on the suction stress of compacted loess and the associated microscopic mechanism. *Water* **13**(13), 2021 (2021).
27. Yuan, K. et al. Influence of dry density and wetting–drying cycles on the soil–water retention curve of compacted loess: experimental data and modeling. *Acta Geotech.* **19**, 1–18 (2024).
28. Ma, T. et al. Microstructural evolution of expansive clay during drying–wetting cycle. *Acta Geotech.* **15**, 2355–2366 (2020).
29. Zhihui, Yuan et al. Multi-scale experiment of mechanical property degradation of a laterite soil under dry-wet cycling. *J. Hydroelectr. Eng.* **41**, 1–13 (2022).
30. Guofang, W. E. I. Study on relationship between shear strength and pore structure of lateritic clay based on NMR. *Yangtze River* **52**(11), 155–160 (2021).
31. Kuan, Liu et al. Multi-scale effects of mechanical property degradation of expansive soils under drying-wetting environments. *Chin. J. Rock Mech. Eng.* **39**(10), 2148–2159 (2020).
32. Yakun, Fan & Zheng Mingxin, Wu. Experimental research on shear strength characteristics of unsaturated coal-bearing soils under dry-wet circulation. *IOP Conf. Ser. Earth Environ. Sci.* **719**(4), 042068 (2021).
33. Yakun, Fan & Zheng Mingxin, Wu. Characteristics for microstructure changes of unsaturated coal-bearing soil under dry-wet circulation. *IOP Conf. Ser. Earth Environ. Sci.* **719**(3), 032037 (2021).
34. GB/T 50123–1999, Geotechnical engineering test method and criterion.
35. Shi, G., Li, X., Guo, Z., Zhang, Z. & Zhang, Y. Effect of mica content on shear strength of the Yili loess under the dry-wet cycling condition. *Sustainability* **14**, 9569 (2022).
36. Huang, X., Zhang, Z., Hao, R. & Guo, Z. The effects of particle gradation on salinized soil in arid and cold regions. *Water* **14**, 236 (2022).

Acknowledgements

This work was supported by the following 2 funds, programs, projects: Scientific Research Programme "Tianshan Excellence":<Mechanisms of coupled geological-hazard-hydrogeological-ecological-environmental feedback of mining on the north slope of Tianshan Mountain and its engineering geological significance>(2023TSYCCX0010), The National Natural Science Foundation of China (42367021), The postgraduate scientific research innovation project "Chain Formation Mechanism and Optimal Prevention Design of Typical Loess Landslide-Debris Flow Disaster Chain in Yili Area" (XJ2025G048).

Author contributions

Conceptualization, M.J. and Z.Z.; Data curation, M.J. and Z.G.; Formal analysis, M.J. and R.L.; Investigation, M.J. and G.S.; Methodology, M.J. and Y.Z.; Project administration, Z.Z.; Resources, Z.Z.; Software, R.L. and J.H.; Supervision, Z.Z.; Validation, G.S., Z.G. and J.H.; Writing—original draft, M.J.; Writing—review & editing, M.J.

Declarations

Competing interests

The authors declare no competing interests.

Additional information

Correspondence and requests for materials should be addressed to Z.Z.

Reprints and permissions information is available at www.nature.com/reprints.

Publisher's note Springer Nature remains neutral with regard to jurisdictional claims in published maps and institutional affiliations.